JOURNAL OF MATERIALS SCIENCE **34** (1999) 4105–4120

Synthesis of aluminum infiltrated boron suboxide drag cutters and drill bits

I. O. KAYHAN, O. T. INAL
Materials & Metallurgical Engineering Department, New Mexico Tech, Socorro, NM 87801, USA

Synthesis of boron suboxide (B_6O) was made by reactive sintering of crystalline boron and zinc oxide powders at 1450 °C, in argon, for 12 h. After sintering, Vickers microhardness testing was performed on the material synthesized and an average hardness value of 34 GPa was obtained. Sintered suboxide (in crushed and ground powder form) was then analyzed through optical and scanning electron microscopies and X-ray diffraction. Following the completion of the analyses, consolidation of the powder was performed. Two different routes were carried out: (1) "explosive consolidation" which was performed in double tube (with a density value of 2.22 g/cm^3) and single tube (with a density value of 2.12 g/cm^3) canister design arrangements and (2) "hot pressing" which was performed in a graphite die assembly, at 1600 °C, in vacuum, for 2 and 4 h (with density values of 2.15 and 2.18 g/cm^3 respectively). Consolidated samples of both routes showed different levels of mechanical attachment, agglomeration, porosity, fracture toughness and fracture strength values, whereas microhardness values and X-ray diffraction plots (as shown in Table I and Figs 6 and 8 respectively) were determined to be similar. Following characterizations, compacts of both routes were then given a high temperature sintering treatment (pressureless sintering) at 1800 °C, in vacuum, for full densification. Both in the "as consolidated" and "densification sintered" stages test results revealed the most desirable and well-established properties for the "explosively consolidated double tube design" compacts (with densification sintered density, microhardness and fracture toughness values of 2.46 g/cm^3, 38 GPa and 7.05 MPa m$^{1/2}$ respectively). Consolidation and desification sintering steps were then followed by a pressureless infiltration step. Aluminum was infiltrated into densification sintered "double tube design consolidated" and "4 h of pressed" samples (better-compacted and better-sintered compacts) in the temperature range 1100–1250 °C, in argon, for 10 h. During infiltrations, the optimum temperature of the infiltration process was determined to be 1200 °C. Characterization results revealed the most uniform and well established properties once more for the double tube design explosively consolidated compact (with aluminum infiltrated density, microhardness and fracture toughness values of 2.55 g/cm^3, 41 GPa and 8.70 MPa m$^{1/2}$ respectively).

1. Introduction

Preparation of materials whose hardnesses are close to that of diamond is challenging since, to date, only cubic boron nitride has been found to compete with diamond and its properties. The approach to the problem is based on crystallochemistry. To build a material with a minimal molar volume, it is necessary to pack as many atoms per unit volume as possible. The requirement of a large number of atoms per unit volume will necessitate larger number of complicated bonds being formed. The sequence of crystal phases, such as grey tin, Ge, Si, and diamond has been found to show this effect. They have molar volumes of 21.5, 14, 12 and 3.4 cm^3 respectively. The value 3.4 cm^3 for diamond (3.5 cm^3 for cubic boron nitride) is the lowest known. However, even at this minimal molar value, the carbon atoms (represented as spheres) making up the diamond structure occupy only 34% of the available space [1].

1.1. Boron and boron systems

Boron has the closest, presently known molar volume (5 cm^3) to that of diamond. Boron and boron rich compounds are attractive systems because of their unique structure, high hardness, high melting point and low density values. Their strong and short covalent bonding provides the basis for a wide range of distinctive refractory, thermoelectric and optical properties as well. Boron exhibits a number of different compositions and structures arising from the specific electronic nature of its atom. Unpaired electrons possessing three bonding functions provide the possibility of forming a series

of electronic configurations of different stabilities. The most important and the most common is the icosahedron, a form that exhibits cubic symmetry [2]. Boron also exists in several phases.

In addition to the crystalline forms of α and β rhombohedral and α and β tetragonal boron, an amorphous form also exists. The temperature, pressure and reactants present during formation determine which phase will result. Each phase exhibits different chemical and physical characteristics. Amorphous boron, which has been deposited at low temperatures, tends to be fine-grained and most reactive. As the temperature rises during deposition, first α-rhombohedral and then β-rhombohedral crystalline material forms. Tetragonal phases are generally formed at intermediate temperatures when impurities are present [2].

Thermodynamically, the most stable form of boron is its β-rhombohedral phase, which possesses a complicated but loosely packed crystal structure composed of B_{12} icosahedra [2]. For many years, studies have been performed for the densification of this stable but loosely packed structure and yet only one approach, based on the creation of interstitial structures (and consequently formation of interstitial bonds), has been found successful [1]. Oxygen atoms dissolving in this electron deficient β-rhombohedral boron structure can be considered a good example for this type bond formation.

Mainly two crystal phases, B_2O and B_6O, have been established to exist on the boron rich side of this boron-oxygen system.

1.2. Boron suboxide system

Boron suboxide (B_6O), with diamond-like properties, was for the first time prepared by Badzian in 1988 [1]. After synthesizing B_6O by means of reactive hot pressing of boron and B_2O_3, he melted the suboxide in an induction furnace, in an inert atmosphere of argon, and characterized its structure and properties. The melted material was found to be black in color with polycrystalline morphology. X-ray diffraction analysis performed on the melt showed the crystallographic structure of the grains to resemble β-rhombohedral boron. By means of chemical analysis (performed by secondary ion mass spectroscopy and Auger electron spectroscopy), boron (being the main ingredient) and oxygen (on the level of 4–5 at %) were detected. Considering the analyzed oxygen percentage, $B_{22}O$ composition was postulated for the melted boron suboxide. The most important conclusion of the study was that melted boron suboxide, with a measured Vickers microhardness value of 59 GPa, was found to easily wear a diamond tip parallel to the (001) plane, or scratch a (111) diamond face in any direction.

1.3. Intent

The intent of this study was to produce cost effective boron suboxide ceramic drag cutters and drill bits to fulfill the needs of the industry on hard rock cutting or drilling applications (instead of the less convenient PDC rock cutters and drills used in today's drilling practice). Boron suboxide is an advanced ceramic material with a high hardness (37 GPa), high melting point (2200–2250 °C), high chemical stability and low theoretical density (2.59 g/cm^3), and it has the potential to be used as an improved ceramic drag cutter or drill bit [3]. However, because of its ceramic nature, it is brittle and has low impact resistance. These concerns of the suboxide compacts were eliminated by means of metal infiltration, resulting in boron suboxide composites having improved mechanical properties (high stability, high fracture toughness and flexural strength values).

2. Experimental

2.1. Boron suboxide synthesis

Boron suboxide was synthesized by reactive sintering of a mixture of crystalline boron (−325 mesh, 95% pure) and zinc oxide (−325 mesh, 100% pure) powders. The first step in the synthesis procedure was the mixing of the two precursor powders in an 8 to 1 mol ratio, to lead to the reaction:

$$8B + ZnO \longrightarrow B_6O + 2B + Zn(g) \uparrow \qquad (1)$$

The homogeneous powder mixture (ball milled for 72 h) was then pressed into (under pressures of 90–130 MPa) cylindrical pellets of 3.05 cm (1.2 in.) in diameter and 1.27 cm (0.5 in.) in thickness, which were consequently sintered at 1450 °C in an argon atmosphere for 12 h (during which time the suboxide reaction took place).

After sintering, the newly synthesized material was crushed and ground into powder form for the subsequent characterization and consolidation steps.

2.2. Consolidation

Consolidations were performed through explosive consolidation and hot pressing routes.

2.2.1. Explosive consolidation

Explosive consolidation was performed in two arrangements; single and double tube canister designs (cylindrical canisters were made of mild steel). In the former case (single tube design arrangement), the powder was vibrationaly packed and pressed directly into the canister (under pressures of 90–100 MPa), whereas, in the second arrangement (see Fig. 1), packing and pressing was performed into a copper tube (under the same pressure) which in turn was placed into the steel canister. In both arrangements, the canisters were sealed with steel top and bottom end plugs.

For both assemblies, ANFO (mixture of ammonium nitrate and fuel oil, with a detonation velocity of 3500 m/s) was selected as the explosive to be used in the system. Upon the detonation of the explosive charge, desired levels of compaction (in an axi-symmetric configuration) were achieved in both geometries.

2.2.2. Hot pressing

Hot pressing of the powder was accomplished in two steps. In the first step a pre-pressing operation was made. The crushed and ground powder was consolidated into cylindrical green pellets of 3.05 cm (1.2 in.) in diameter and 5.08 cm (2 in.) in thickness. The

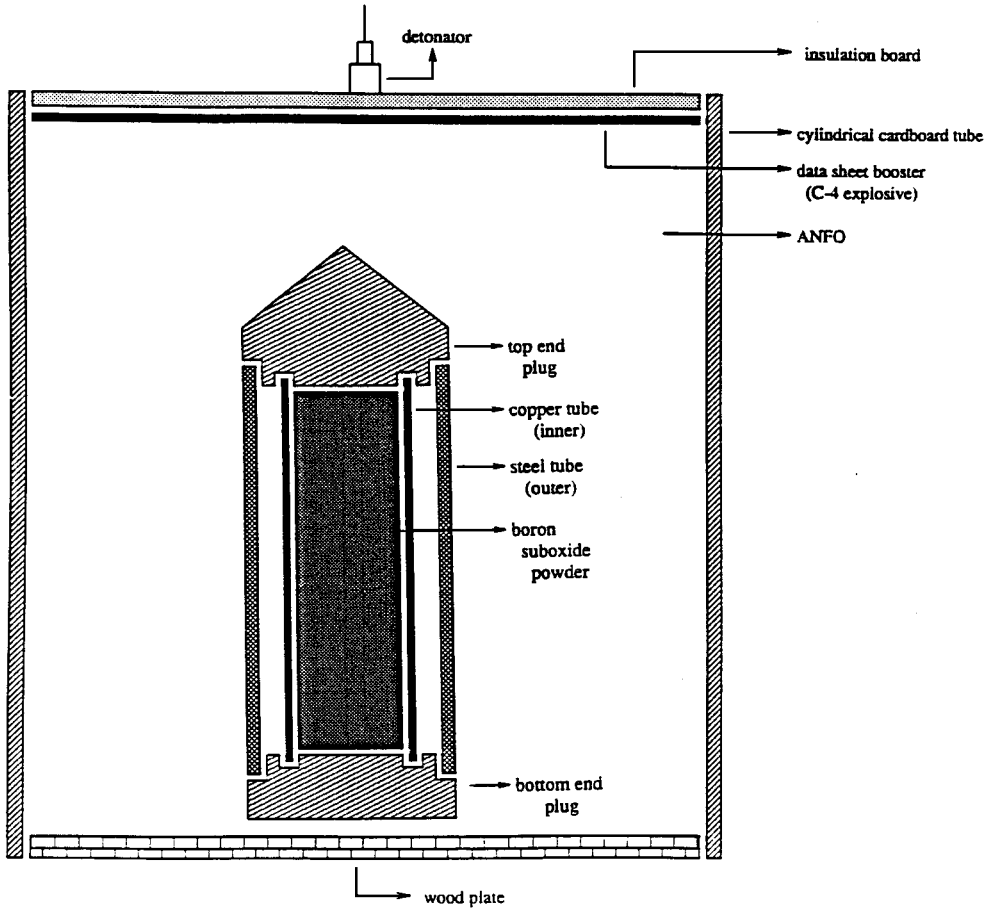

Figure 1 Cylindrical, axi-symmetric double tube explosive consolidation setup (P. 7).

second step was the conventional hot pressing operation performed under vacuum using an inductively heated graphite die with an inside diameter of 3.56 cm (1.4 in.). In this step, an intermediate barrier layer of boron nitride was provided between the green sample and the graphite die and rams to prevent carbon diffusion from the graphite to the sample. Hot pressings were made at 1600 °C under 40 MPa pressure for 2 and 4 h respectively. During pressing, pressure was maintained at 10 MPa up to the sintering temperature and then was increased to 40 MPa. A schematic of the die assembly can be seen in Fig. 2.

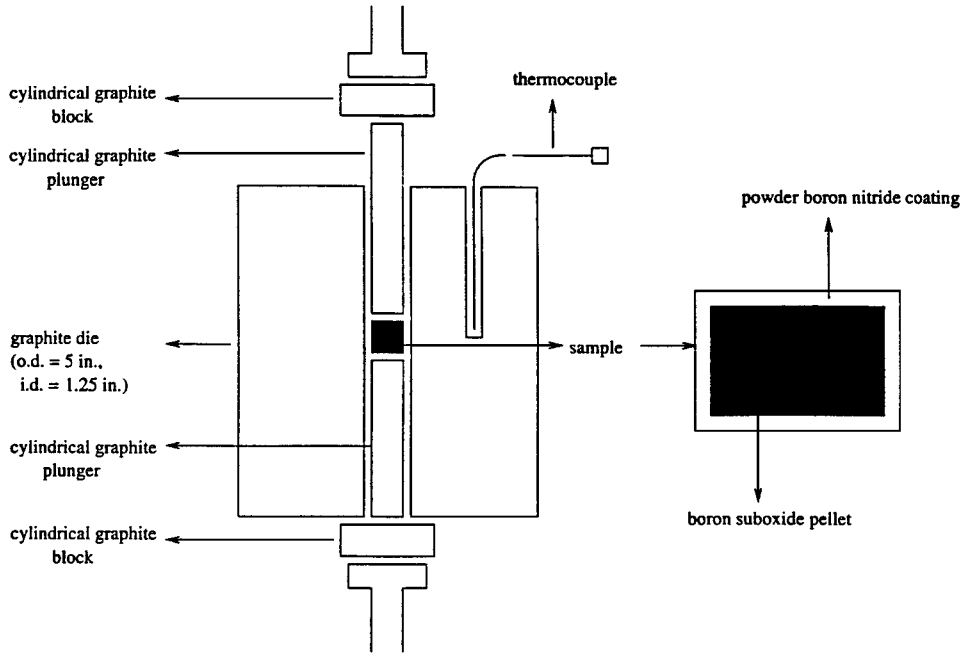

Figure 2 The schematic diagram of the hot pressing die assembly. The green sample coated with boron nitride is also shown in the figure (P. 7).

2.3. Densification sintering

Following consolidation, compacts of both routes were given a high temperature heat treatment at 1800 °C under vacuum with no pressure applied. Samples were sintered at this temperature for 2 h for full densification.

2.4. Aluminum infiltration

Infiltrations were carried out in a tube furnace, in the temperature range of 1100–1250 °C, in pure argon atmosphere, with no external pressure applied. Pure aluminum (99.99%) was selected as the metal to be infiltrated, wherein, because of their better density, fracture toughness, flexural strength and lower % porosity values, densification sintered "double tube design explosively consolidated" and "4 h of hot pressed" pellets were selected as the compacts to receive the infiltrations.

"Capillary tube action" technique was followed to achieve the infiltrations (aluminum filling the internal voids of the sintered compacts). Suboxide samples (cylindrical pellets having 3.8 cm (1.5 in.) lengths) were placed on top of pieces of solid aluminum that were ground, polished and ultrasonically cleaned. The aluminum pieces, with suboxide samples on top of them, were then placed into alumina crucibles that were placed into the hot zone of the tube furnace (where the infiltrations were to be performed). Before starting each infiltration cycle, the tube was sealed at both ends, was fully evacuated and subsequently purged with argon to ensure a pure, inert atmosphere in the system.

The time needed for each infiltration cycle (in terms of the desired height of infiltration, 3.8 cm) was calculated as 10 h (depending on a minimized critical pore radius estimation). For optimization of the infiltration temperature, infiltrations were carried out at 1100, 1150, 1200 and 1250 °C for each design compact.

2.5. Characterizations

2.5.1. Synthesized material

Following synthesis, Vickers microhardness testing was performed on randomly selected samples of the reactively sintered material (representing each sintering cycle). Hardness values were obtained from sample surfaces that were ground and polished, with 100 g of load applied. For an average value determination, four indentations were taken from each sample surface.

After hardness value determinations, all successfully sintered pellets were crushed and ground into powder form for the subsequent X-ray diffraction, optical microscopy and scanning electron microscopy analyses and characterizations.

In order to delineate boron suboxide formation, powder material was given a qualitative XRD analyses. Randomly selected powder samples, representing each sintering cycle, were analyzed in the 10°–100° 2θ range, under CuK_α radiation. The composition of the synthesized material was then determined through the quantitative analysis of the gathered X-ray diffraction data.

Knowing that it was composed of only boron and oxygen (no extraneous element was detected in its composition), elemental compositional analysis was performed on the crushed and ground powder. The % composition values obtained through the quantitative X-ray diffraction analysis of the powder material was taken as the reference point, and from that, by means of a series of calculations, an elemental composition was derived.

Following XRD analyses, optical and scanning electron microscopies were carried out to characterize the size and geometry of the crushed and ground powder particles.

2.5.2. Consolidated samples

From recovered compacts of all four designs, small samples (1 in. long) were sliced and metallographically prepared for further density, porosity (open and closed), microhardness, X-ray diffraction and optical and scanning electron microscopy characterizations.

Bulk densities were determined according to ASTM Standard C 20. Using the measured dry, suspended and saturated weight values, the density of each sample was ascertained according to the following equation:

$$\text{Bulk Density (g/cm}^3) = [D/(W - S)] \tag{2}$$

After density measurements, using Equations 3 and 4 (according to ASTM Standard C 20), apparent and closed porosity values (%) were determined for each specimen.

$$\text{Apparent Porosity (\%)} = [(W - D)/(W - S)] \times 100 \tag{3}$$

$$\text{Closed Porosity (\%)} = [(D - S)/(W - S)] \times 100 \tag{4}$$

where D, S and W represent the dry, suspended and saturated weights of the samples respectively.

Following % porosity calculations, Vickers microhardness test, X-ray diffraction, optical and scanning electron microscopy analyses were made on the consolidated samples. In addition to these tests, the compacts were characterized through three-point bend testing for fracture toughness (according to ASTM Standard E 399) and flexural strength (according to ASTM Standard C 293) determinations.

Fracture toughness values were evaluated on specimens that were cut 2 mm through the height (using a 0.635 mm thick diamond blade), in the center of the span, to simulate a crack opening. The equation used to calculate the fracture toughness of the specimens is:

$$K_{\text{IC}} = (3SP/2BW^{3/2})c^{0.5}F(\alpha) \tag{5}$$

where:

$$\alpha = c/W \tag{6}$$

$$F(\alpha) = [1.99 - \alpha(1 - \alpha) \times (2.15 - 3.93\alpha + 2.7\alpha^2)]/[(1 + 2\alpha)(1 - \alpha)^{3/2}] \tag{7}$$

The flexural strength values (MPa) of the uncracked specimens were determined according to the following equation:

$$\text{Flexural Strength} = [3SP]/[2BW^{3/2}] \qquad (8)$$

where P is maximum load at the breakage (N) W the specimen height (mm) B the specimen width (mm) S the span length (mm) and c is the crack length (mm).

2.5.3. Densification sintered and aluminum infiltrated samples

The above stated characterizations were also made on all compacts (of both routes) following densification sintering and aluminum infiltration steps.

3. Results

3.1. Boron suboxide synthesis

Boron suboxide was successfully synthesized at 1450 °C, in argon atmosphere, through reactive sintering of the precursor powders for 12 h. In addition to the actual sintering temperature of 1450 °C, synthesis was achieved with success also at 1250, 1300, 1350 and 1400 °C. The final product of all these sintering cycles, regardless of the different sintering temperature conditions, were observed to be always a reddish-brown colored, highly sintered material with an average Vickers microhardness value of 34 GPa.

X-ray diffraction data obtained from the sintered materials were found to match the previously determined patterns for boron suboxide, B_6O (see Fig. 3). There were only a few extra peaks observed in the powder patterns that were determined to be the peaks of rhombohedral boron (free boron) and boron oxide (B_2O_3). By quantitative analysis of the gathered XRD data, 1450 °C sintered material was determined to be composed of 80.5 wt % B_6O, 14.5 wt % boron (rhombohedral) and 5 wt % boron oxide (a total of 80.6 wt % of boron and 19.4 wt % oxygen). There were no zinc or zinc oxide peaks determined in the examined patterns.

By means of optical and scanning electron microscopy analyses, 1450 °C sintered material, which was crushed and ground into powder form, was determined to be composed of irregular and non-symmetric shaped particles (in the form of cubic, tetrahedral and spherical structures, etc.) that were spread into a very large size range (between 600 microns and 1 micron in length). The optical and scanning electron micrographs of the powder material can be observed in Figs 4a and b respectively.

3.2. Explosive consolidation

Upon the detonation of the explosive charge (the same type and amount of explosive used for both arrangements), the single tube canister geometry was observed to experience a 14.2% shrinkage, whereas, the double tube canister arrangement was determined to experience a 17.7% truncation. In light of these shrinkage values, the double tube design compact (with a measured density value of 2.22 g/cm^3) was determined to be denser than the single tube design compact, which was measured to have a density value of 2.12 g/cm^3. Through optical microscopy, the single tube design compact was determined to have a rough consolidation surface (composed of particles in a size range of 6–0.2 μm), whereas the double tube design compact was determined to possess a smoother surface (composed of particles in a narrower size range of 0.65–0.2 μm).

By means of scanning electron microscopy, a non-uniform mixture of mechanically attached large and small sized powder particles was observed for the single tube design compact, whereas, a uniform mixture of relatively smaller sized and fairly well attached powder particles was seen to exist for the double tube design compact. For both consolidation arrangements, particle

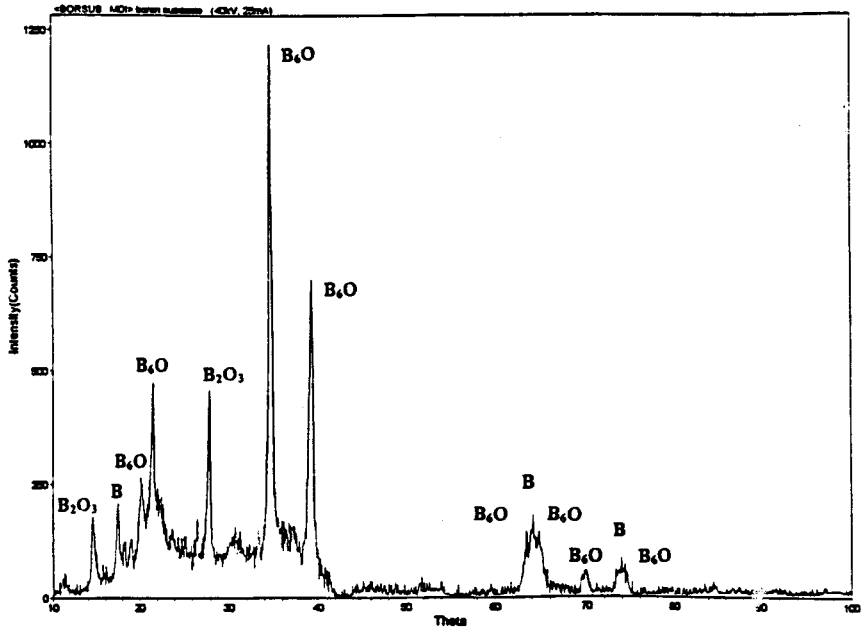

Figure 3 XRD pattern obtained from the reactively sintered material (P. 12).

(a)

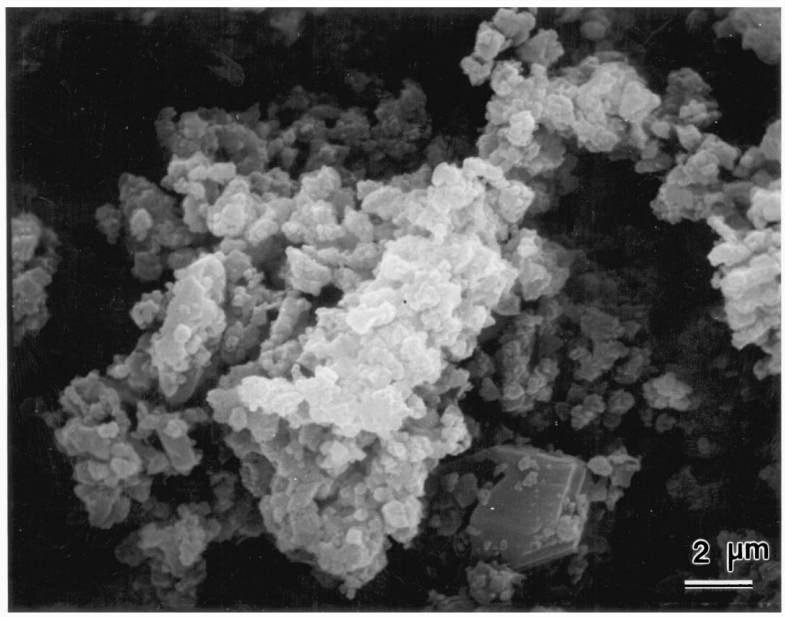

(b)

Figure 4 (a) OM and (b) SEM micrographs of the synthesized material (in powder form) (P. 12).

geometries were examined to be uniform (symmetrical spherical shapes) with the sharp corners and edges of the particles being all deformed and rounded as a consequence of the shock waves traveling through the powder materials. The optical and scanning electron micrographs of the double tube design explosively consolidated compact can be observed in Figs 5a and b respectively.

Through Vickers microhardness testing, the same average hardness value of 35 GPa was evaluated for the compacts of both geometries.

Through three-point bend testing, double tube design compact was determined to have better fracture toughness (average values of 5.99 vs. 4.95 MPa $m^{1/2}$) and flexural strength (average values of 64.03 vs. 52.98 MPa) than the single tube design compact.

X-ray diffraction patterns of the compact bodies (see Fig. 6) were observed to be different than the patterns of the powders prior to consolidation. The changes observed were related to the boron oxide (B_2O_3) peaks, which were determined to be shorter in this pattern. By quantitative analysis of the XRD data, the amounts of phases present in the compacts were determined to be 81.5 wt % boron suboxide, 15.5 wt % boron and 3 wt % boron oxide for consolidated bodies of both geometries.

3.3. Hot pressing

The compact that was hot pressed for 4 h was measured to be denser than the one that was hot pressed for 2 h (with density values of 2.18 and 2.15 g/cm^3 respectively). Through scanning electron microscopy,

(a)

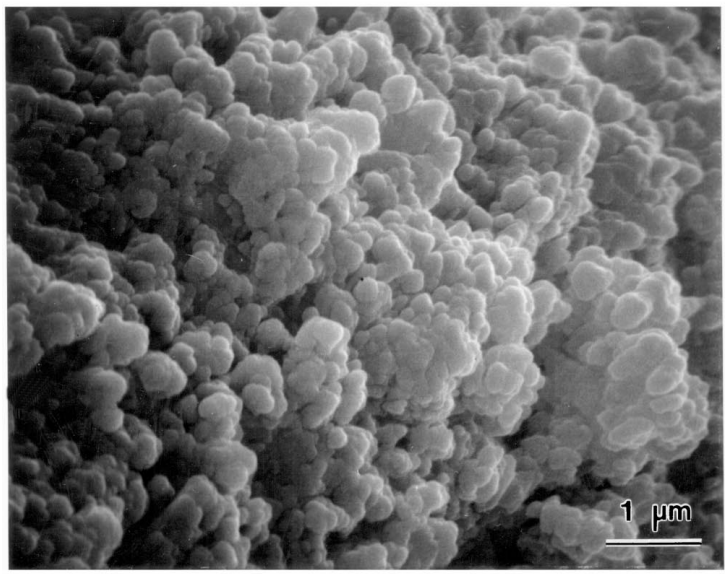

(b)

Figure 5 (a) OM and (b) SEM micrographs of the double tube design explosively consolidated compact (P. 13).

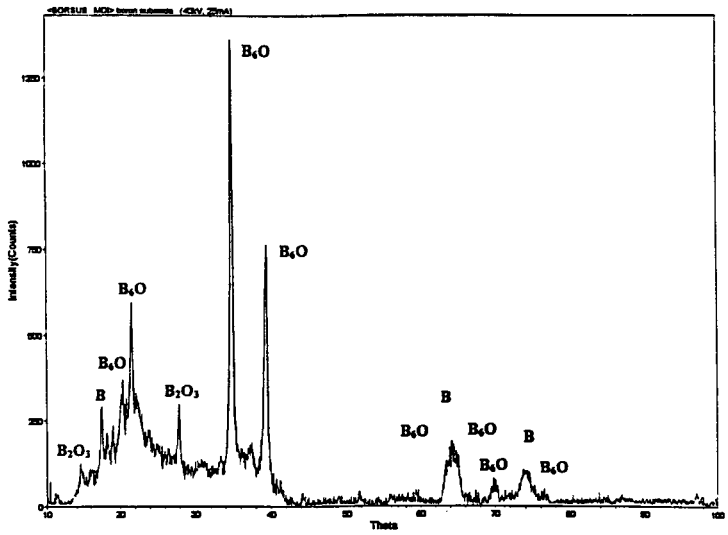

Figure 6 XRD pattern obtained commonly from compacted samples of both single and double tube design consolidations (P. 14).

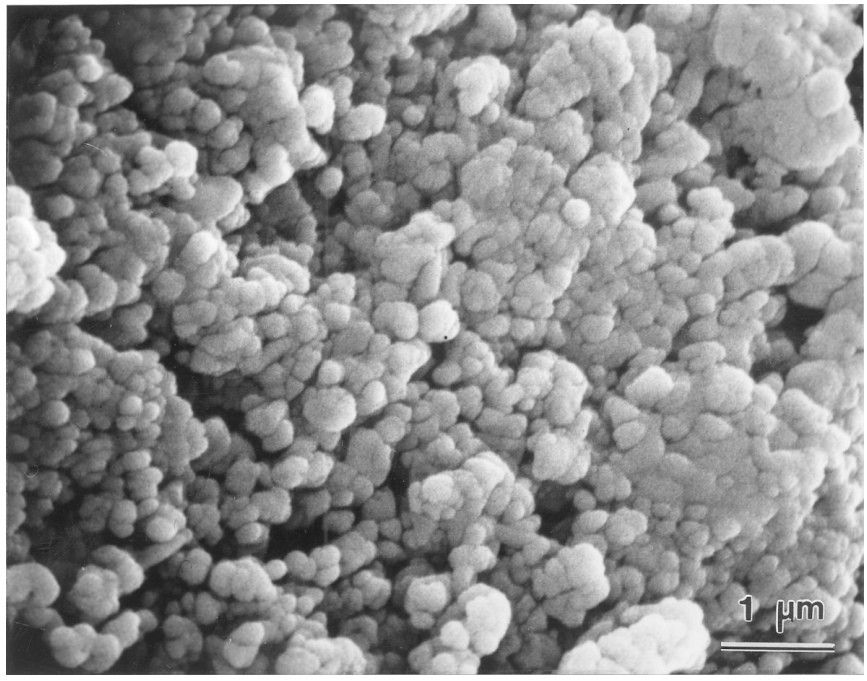

Figure 7 SEM micrograph of the 4 h of hot pressed compact (P. 14).

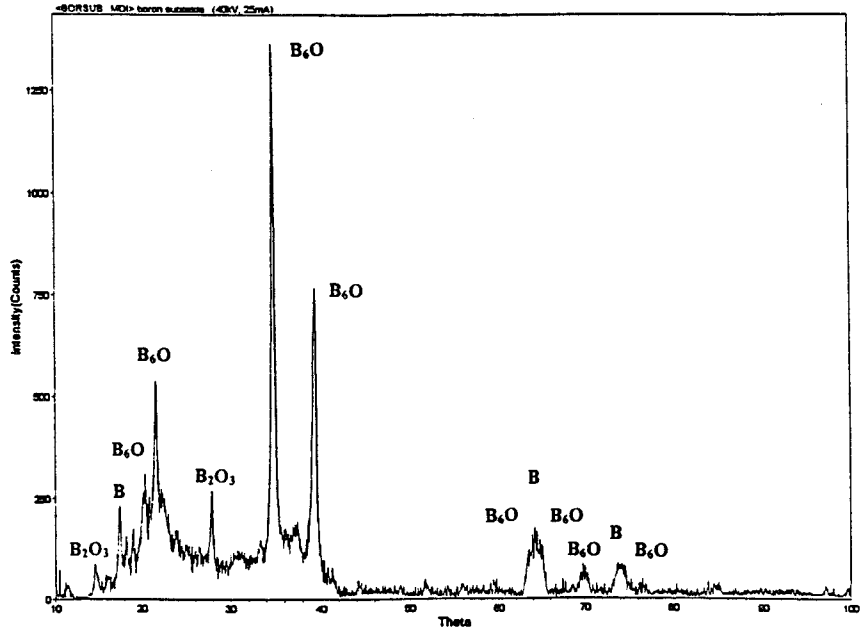

Figure 8 XRD pattern obtained commonly from both 2 and 4 h of hot pressed samples (P. 15).

a structure composed of a mixture of relatively large and small sized powder particles (in a size range of 2.2–0.2 μm), which showed a low level of mechanical attachment, was observed for the sample hot pressed for 2 h, whereas, a more uniform mixture of relatively smaller sized particles (in a size range of 1–0.2 μm), which showed a higher level of attachment, was observed for the sample hot pressed for 4 h (see Fig. 7). In both samples, particle geometries were observed to be uniform (spherically shaped particles).

Through Vickers microhardness testing, the same average hardness value of 35 GPa was calculated for hot pressings of both durations.

Through three-point bend tests, the sample hot pressed for 4 h was determined to have better fracture toughness (average values of 5.52 vs. 5.35 MPa $m^{1/2}$) and flexural strength (average values of 59.07 vs. 57.18 MPa) than the sample hot pressed for 2 h.

X-ray diffraction patterns of the hot pressed compacts (see Fig. 8) were seen to be very similar to the patterns obtained from the analyses of the explosively consolidated solid bodies. In these patterns, the boron oxide peaks were also observed to be shorter. By quantitative analysis of the XRD data, the amounts of phases present in the hot pressed compacts of both durations were determined to be 82 wt % boron suboxide, 15 wt % boron and 3 wt % boron oxide.

3.4. Densification sintering

Results of the density measurements showed that the double tube design compact was denser than all the others (single tube design compact and 2 and 4 h of hot

TABLE I Density (±0.5%), hardness (±1%), average fracture toughness (±0.5%), average flexural strength (±2.5%), % open (±0.5%) and closed (±0.05%) porosity values of the material synthesized; (a) after synthesis, (b) after consolidation, and (c) after densification sintering stages

	Density (g/cm^3)	Hardness (GPa)	Fracture toughness (MPa m$^{1/2}$)	Flexural strength (MPa)	Porosity (%)	
					Open	Closed
Synthesized material	—	34	—	—	—	—
			Consolidated values			
Single tube design	2.12	35	4.95	52.98	15	
2 h of hot pressing	2.15	35	5.35	57.18	13	
4 h of hot pressing	2.18	35	5.52	59.07	10.5	
Double tube design	2.22	35	5.99	64.03	9	
			Densification sintered values			
Single tube design	2.28	36	5.54	59.22	12	
2 h of hot pressing	2.31	36	5.84	62.43	10.5	
4 h of hot pressing	2.39	37	6.23	66.70	7.5	
Double tube design	2.46	38	7.05	75.44	5	

pressed compacts) with a measured value of 2.46 g/cm^3 (closest value to the theoretical density value of B_6O, 2.59 g/cm^3 [3]). Density values of all compacts can be observed in Table I. Scanning electron microscopy analyses revealed that all compacts had different structures. Single tube design compact was determined to have a rather porous but well sintered structure. The sample hot pressed for 2 h, in contrast, was observed to be composed of a less porous but moderately sintered structure. Comparing to these two, the sample hot pressed for 4 h was determined to have both a less porous and a better sintered structure (see Fig. 9). As was predicted, the double tube design compact was determined to have the most uniform and well sintered structure with the least porosity (see Fig. 10). The porosity levels recognized in all these compacts can be seen in Table I.

Through Vickers microhardness tests, the average hardness values of the single tube design and hot pressed (for 2 h) compacts were both determined to be 36 GPa, whereas the average hardness value of the compact sample hot pressed for 4 h was observed to be around 37 GPa. The double tube design compacted sample was determined to have the highest average hardness value, 38 GPa, among others.

By means of three-point bend testing, double tube design compact was determined to possess the highest fracture toughness (an average value of 7.05 MPa m$^{1/2}$) and flexural strength (an average value of 75.44 MPa) among others. Measured fracture toughness and flexural strength values of all compacts can be observed in Table I.

Both explosively consolidated and hot pressed samples were observed to exhibit the same X-ray diffraction pattern (see Fig. 11), which is different than the ones obtained from explosively consolidated and hot pressed compacts prior to the sintering step. The changes observed were basically related to the boron peaks. All boron peaks in the structures were observed to belong to tetrahedral boron. It should also be noted that, no

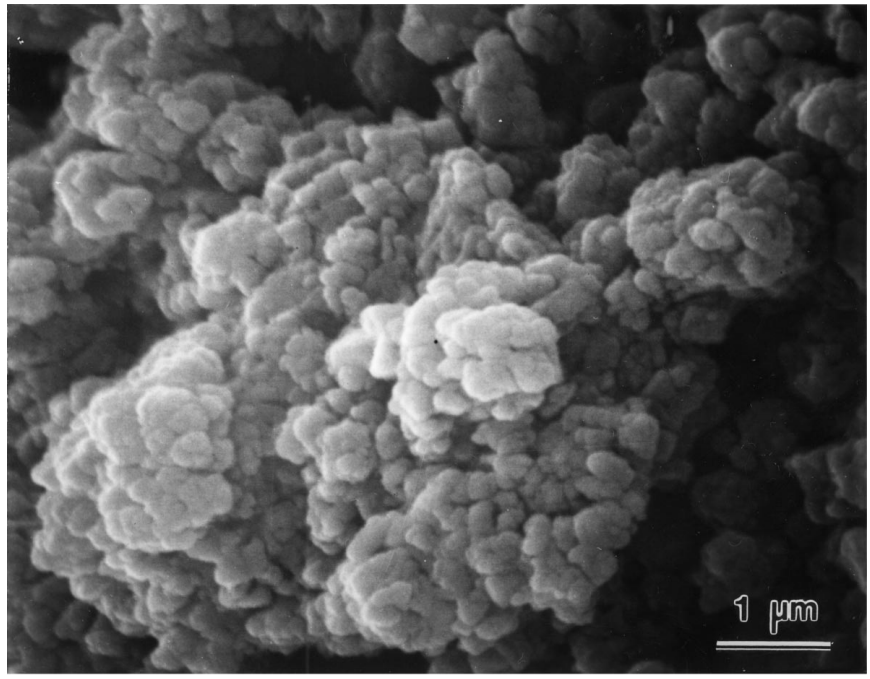

Figure 9 SEM micrograph of the densification sintered sample of 4 h of hot pressed compact (P. 15).

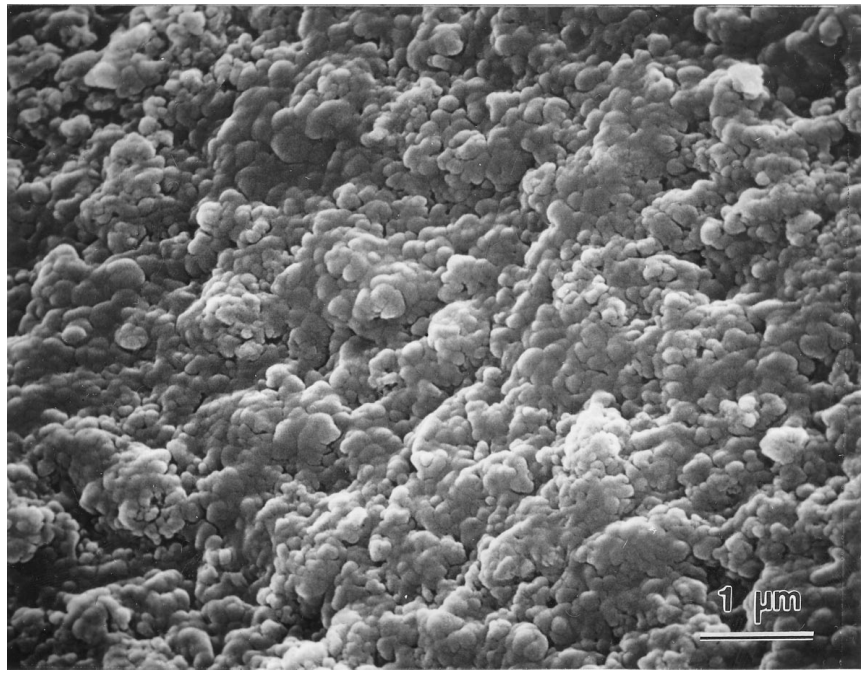

Figure 10 SEM micrograph of the densification sintered sample of double tube design compact (P. 16).

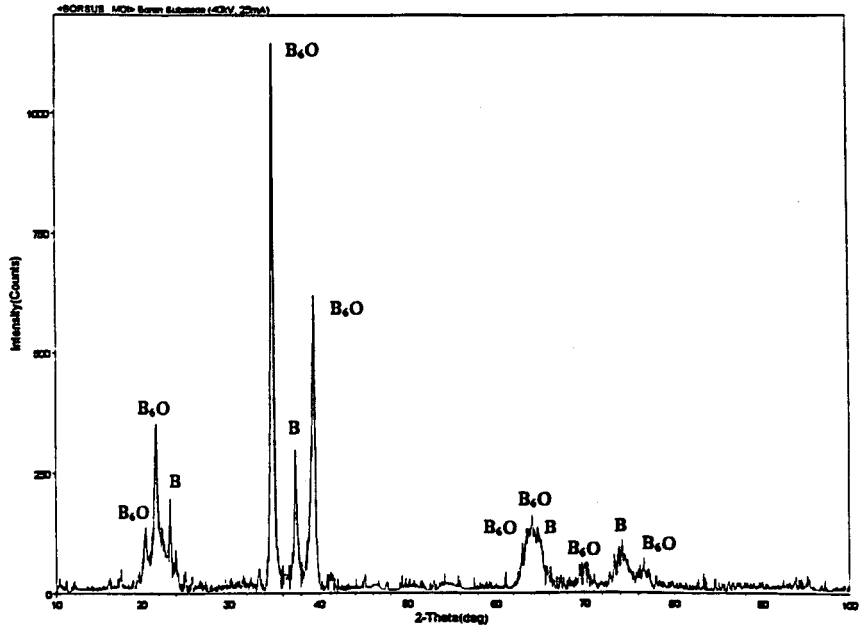

Figure 11 XRD plot obtained commonly from densification sintered samples of both explosively consolidated and hot pressed compacts (P. 16).

boron oxide (B_2O_3) peaks were seen in this pattern. By quantitative analysis of the XRD data, the amounts of phases present in the compacts were determined to be 83 wt % boron suboxide and 17 wt % boron.

3.5. Aluminum infiltration

Bulk density measurements revealed that aluminum infiltrated samples of both "double tube design explosively consolidated" and "4 h of hot pressed compacts" had quite similar density values in the 1100–1250 °C infiltration range (listed in the order of increasing infiltration temperature in Table II). From these measured values, the ones obtained from the 1200 °C infiltrated compacts were determined to be the highest. Through porosity and Vickers microhardness measurements, 1200 °C infiltrated compacts (of both route consolidations) were also determined to possess the lowest apparent and closed porosity and highest microhardness values (values listed in the order of increasing

TABLE II Bulk density values of the infiltrated samples of "double tube design explosively consolidated" and "4 h of hot pressed" compacts in 1100–1250 °C temperature range

	Density (g/cm^3) (±0.5%)	
Infiltration temperature (°C)	Explosively consolidated samples	Hot pressed samples
1100	2.49	2.48
1150	2.52	2.49
1200	2.55	2.53
1250	2.53	2.51

TABLE III Apparent and closed porosity values of infiltrated (in 1100–1250 °C temperature range) compacts of both design consolidations

Infiltration temperature (°C)	Apparent porosity (%) (±0.5%)		Closed porosity (%) (±0.05%)	
	Explosively consolidated	Hot pressed	Explosively consolidated	Hot pressed
1100	3.85	4.25	0.70	0.82
1150	2.70	3.85	0.49	0.70
1200	1.55	2.30	0.25	0.40
1250	2.30	3.10	0.40	0.54

TABLE IV Average Vickers microhardness values of the infiltrated samples of "double tube design explosively consolidated" and "4 h of hot pressed" compacts in 1100–1250 °C temperature range

Infiltration temperature (°C)	Vickers microhardness (GPa) (±1%)	
	Explosively consolidated samples	Hot pressed samples
1100	28	25
1150	40	38
1200	41	40
1250	40	39

TABLE V "Fracture Toughness" values of the infiltrated compacts of both design consolidations

	Fracture Toughness (MPa $m^{1/2}$) (±0.5%)	
	Explosively consolidated samples	Hot pressed samples
1100 °C Infiltrations		
1st specimen	5.28	4.96
2nd specimen	5.44	5.04
3rd specimen	5.70	5.11
Average	5.47	5.04
1150 °C Infiltrations		
1st specimen	7.93	6.98
2nd specimen	8.08	7.11
3rd specimen	7.97	7.14
Average	7.99	7.08
1200 °C Infiltrations		
1st specimen	8.69	8.09
2nd specimen	8.68	8.17
3rd specimen	8.74	8.11
Average	8.70	8.12
1250 °C Infiltrations		
1st specimen	8.49	7.98
2nd specimen	8.38	7.92
3rd specimen	8.53	7.84
Average	8.47	7.91

TABLE VI "Flexural Strength" values of the infiltrated compacts of both design consolidations

	Fracture Strength (MPa) (±2.5%)	
	Explosively consolidated samples	Hot pressed samples
1100 °C Infiltrations		
1st specimen	56.47	53.05
2nd specimen	58.18	53.90
3rd specimen	60.96	54.65
Average	58.54	53.87
1150 °C Infiltrations		
1st specimen	84.81	74.65
2nd specimen	86.42	76.04
3rd specimen	85.24	76.36
Average	85.49	75.68
1200 °C Infiltrations		
1st specimen	92.94	86.52
2nd specimen	92.83	87.38
3rd specimen	93.48	86.74
Average	93.08	86.88
1250 °C Infiltrations		
1st specimen	90.80	85.35
2nd specimen	89.63	84.71
3rd specimen	91.23	83.85
Average	90.55	84.64

temperature in Tables III and IV respectively) among others.

Optical microscopy of compacts infiltrated at 1200 °C (determined to be the best) revealed that both "double tube design explosively consolidated" and "4 h of hot pressed" compacts had very uniform and smooth surface structures, with aluminum being infiltrated into every apparent pore around the compacts (see the micrographs of the compact surfaces in Figs 12a and b, bright spots observed all over the structures are the aluminum infiltrated regions). In both design compacts the rough nature of the consolidated surfaces (caused by the non-uniform, large and small sized, agglomerated powder particles) were observed to be no longer recognizable.

Scanning electron microscopy (see the micrographs of the compacts of both design consolidations in Fig. 13) revealed that infiltrated "double tube design explosively consolidated" and "4 h of hot pressed" samples both had quite uniform and well-sintered structures with very low closed porosity levels (within the 0.25–1% range). Aluminum was seen to have infiltrated almost everywhere in and around the compacts (all of the open and closed pores in the structures being filled with the infiltrant aluminum metal). The very large open pores that can be observed in some parts of the micrographs are characteristic features of the fracture surfaces of the samples.

Through three-point bend testing, 1200 °C infiltrated compacts (of both routes) were determined to possess the highest fracture toughness and flexural strength values (values listed in the order of increasing temperature in Tables V and VI respectively). Except for the very low toughness and strength values obtained from the 1100 °C infiltrated samples, the fracture toughness and flexural strength values of the compacts infiltrated at the temperatures of 1150, 1250 °C were also determined to be satisfactory.

X-ray diffraction data of both route compacts (explosively consolidated and hot pressed) were determined to exhibit nearly the same pattern for the infiltrations carried out at 1150, 1200 and 1250 °C temperatures. Considering that the highest density, highest hardness and lowest porosity values were obtained from the compacts infiltrated at 1200 °C, the patterns obtained from them were selected to be qualitatively and quantitatively

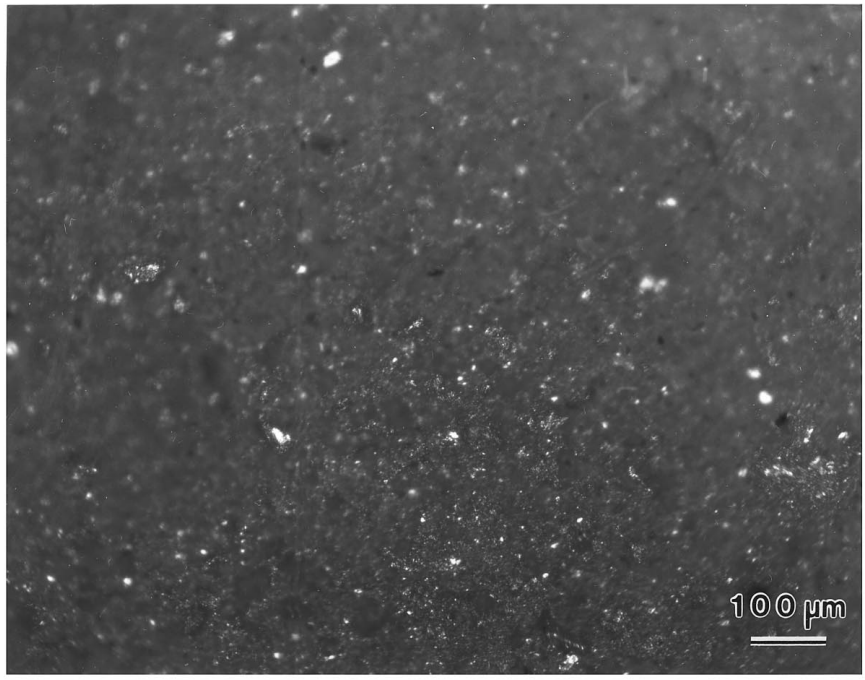

(a)

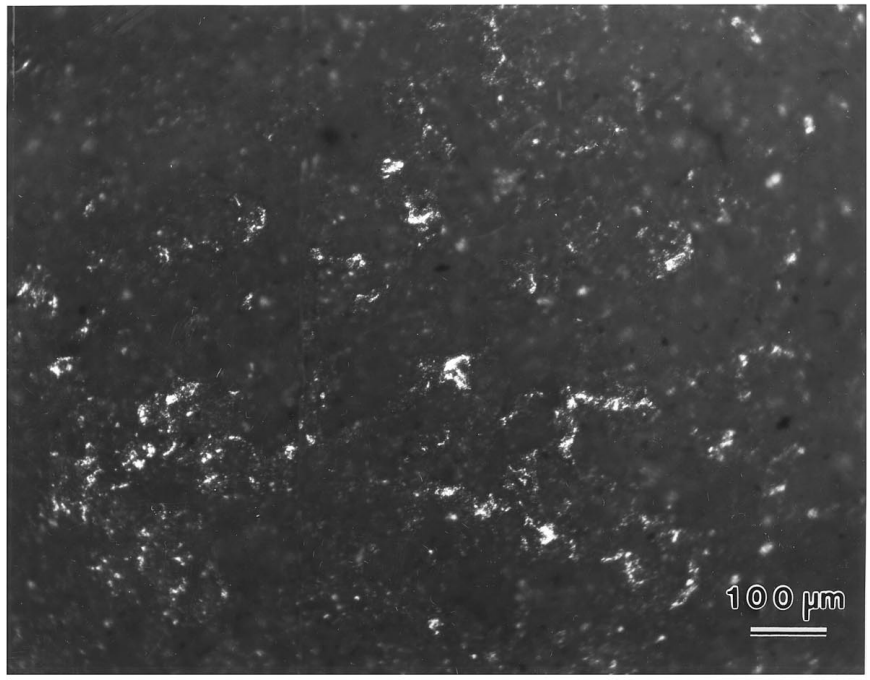

(b)

Figure 12 OM micrographs of 1200 °C aluminum infiltrated samples of (a) "double tube design explosively consolidated" and (b) "4 h of hot pressed" compacts (P. 17).

analyzed (see the patterns of both route compacts, infiltrated at 1200 °C, in Figs 14 and 15 respectively). Both patterns were observed to be quite different from the patterns obtained from both route compacts prior to the aluminum infiltration step. First of all, numerous aluminum oxide (Al_2O_3) and aluminum borate ($Al_{1.67}B_{22}$) peaks were observed in the data, and secondly, all of the free boron peaks (determined previously in the patterns of the densification sintered compacts) were seen to have been obviated from the structures, with boron suboxide phase still being the main constituent. By quantitative analysis of the XRD data, the amounts of phases present in the explosively consolidated and hot pressed compacts were determined to be 69 wt % boron suboxide, 17 wt % aluminum borate, 14 wt % aluminum oxide, and, 71 wt % boron suboxide, 16 wt % aluminum borate, 13 wt % aluminum oxide respectively.

Unlike the patterns obtained from 1150, 1200 and 1250 °C infiltrations, the diffraction data obtained from the compacts infiltrated at 1100 °C were determined to reveal a different pattern (see the pattern obtained for both route compacts in Fig. 16). Both the explosively

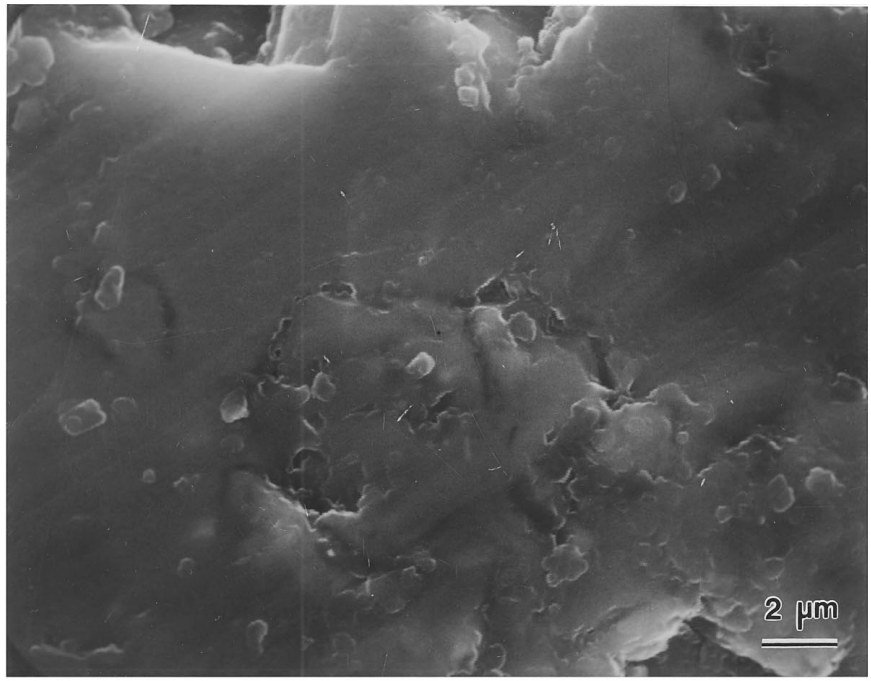

(a)

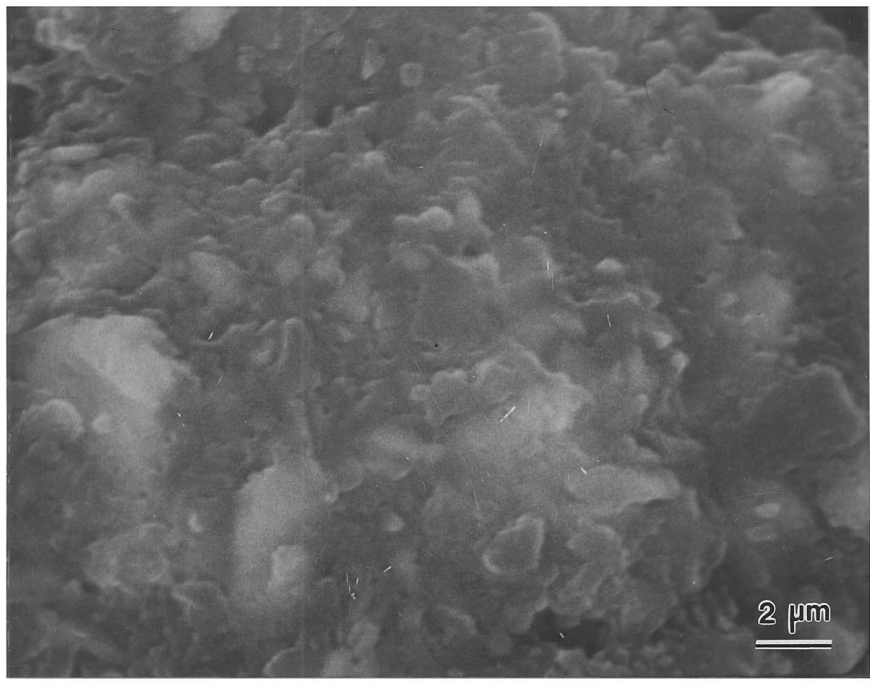

(b)

Figure 13 SEM micrographs of 1200 °C aluminum infiltrated samples of (a) "double tube design explosively consolidated" and (b) "4 h of hot pressed" compacts (P. 17).

consolidated and hot pressed samples were observed to exhibit the same diffraction pattern in which the main constituents were determined to be 4 different kinds of aluminum borate phases ($Al_5(BO_3)O_6$, $Al_4B_2O_9$, $Al_{18}B_4O_{33}$, $Al_{1.67}B_{22}$) and an aluminum oxide (Al_2O_3) phase.

4. Discussions

Average Vickers microhardness values of the synthesized material (34 GPa), explosively consolidated compacts (35 GPa) and hot pressed samples (35 GPa) were found to be lower than the previously reported hardness value (37 GPa) of the boron suboxide compound [3]. The reasons for such low values are assumed to be the presence of excessive porosity and boron oxide phase in the structures.

Although the same amount of explosive was used with the same detonation geometry in both single and double tube design setups, the percentage of shrinkage and compact density values obtained with the double

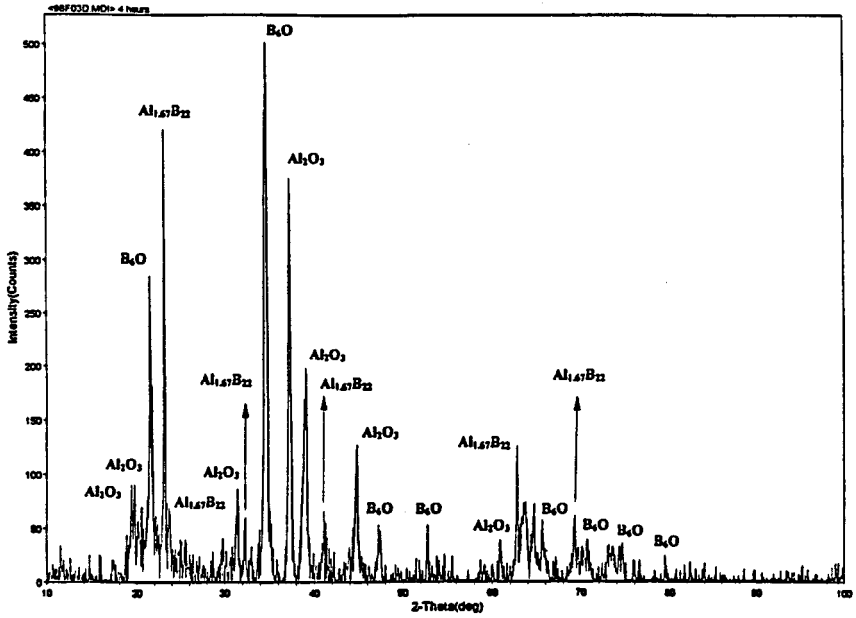

Figure 14 XRD pattern of the aluminum infiltrated (at 1200 °C) sample of "4 h of hot pressed" compact (P. 18).

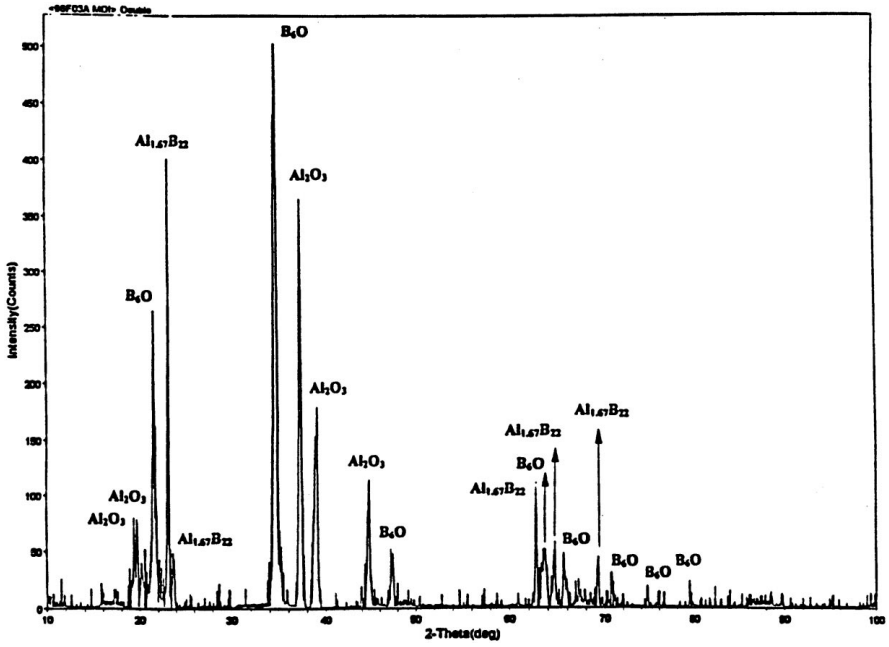

Figure 15 XRD pattern of the aluminum infiltrated (at 1200 °C) sample of "double tube design explosively consolidated" compact (P. 18).

tube design was greater. This significant structural difference is assumed to be due to the higher pressures and higher pulse durations utilized by the flyer tube (double tube) design.

During characterizations, 2 and 4 h of hot pressed samples were both observed to be not quite well sintered under the conditions at which hot pressings were performed. The reason is assumed to emanate from: (1) temperature limitations of the hot pressing assembly (1600 °C) and (2) low pressures (40 MPa) applied during the pressings. Despite being not well sintered, the density of the compact that was hot pressed for 4 h was observed to be greater than that for the 2 h sample. The reason for this difference could be the longer pressing duration accomplished in the former case.

In XRD patterns of explosively consolidated and hot pressed samples, the peak heights of the boron oxide (B_2O_3) phase were determined to be diminished in comparison to the heights observed in the XRD plots of the powders prior to consolidation. This is assumed to be due to the decomposition of the boron oxide powder, to some extent, into boron suboxide and boron (rhombohedral) in both routes of consolidations.

Evaluation of the XRD data of the densification sintered compacts revealed that samples of both route consolidations experienced the same structural change of "transformation of rhombohedral boron into tetrahedral boron" during the sintering processes. Almost all of the rhombohedral boron, present in the as consolidated structures, was seen to have transformed into tetrahedral boron.

Densification sintered compacts of both route consolidations were observed to have the same composition (determined by quantitative analyses of their XRD

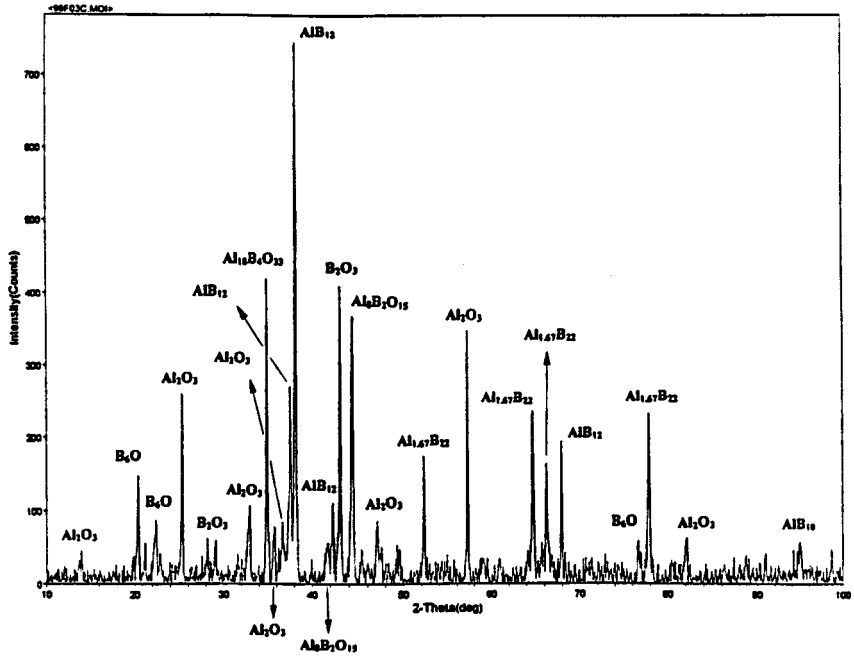

Figure 16 Typical XRD pattern for both explosively consolidated and hot pressed compacts that were aluminum infiltrated at 1100 °C (P. 19).

data), but different hardness values. The reason for this difference is assumed to be due to the various amounts (%) of open and closed porosities determined in their structures, whereas, the increase in hardness values of the compacts, from the as consolidated values to the densification sintered values, is assumed to be due to (1) densification sintering of the samples, i.e. reduced porosity, etc., and (2) structural change that boron experienced in all samples.

Although densification sintered double tube design sample had the highest density and lowest apparent porosity values, it was observed to possess a higher closed porosity value than the 4 h of hot pressed sample. The reason why such a lower value was obtained is believed to be possibly due to the presence of transverse and radial cracks introduced into the core of the compact during explosive consolidation.

Other than the 1200 °C infiltrations, the compacts infiltrated at 1150 and 1250 °C were also determined to possess optimum properties (high density, high microhardness, low apparent and closed porosity values, etc.). However, the compacts infiltrated at 1100 °C were observed to have inferior properties to the others. From the XRD data, it is assumed that oxidation had taken place in the tube furnace during the infiltrations carried out at this temperature, i.e. free oxygen in the system causing the dissolution of the suboxide phase into boron oxide phase and possibly limiting the infiltration of aluminum into the compacts resulting in inferior properties.

Aluminum was determined (through optical microscopy) to have infiltrated into double tube design explosively consolidated compacts to a very high level (during all 1150, 1200 and 1250 °C infiltrations). Extensive infiltration of aluminum into these highly sintered compacts is believed to have taken place through capillary channels, having radii in the vicinity of R_c (having a postulated value of 0.05 μm in highly sintered materials [5]), that connected the closed porosities in the samples to the apparent porosity sites around the compacts. The reductions achieved in the porosity levels of the structures and also the generated interfaces (between suboxide-alumina-aluminum borate phases) are assumed to have resulted in infiltrated compacts having high hardness, density, toughness values, etc.

5. Conclusions

Boron suboxide was successfully synthesized by reactive sintering of crystalline boron and zinc oxide precursor powders. Both "explosive consolidation" and "hot pressing" techniques were proved to be applicable for the consolidation of the synthesized suboxide powder.

Consolidations, achieved through both explosive consolidation and hot pressing routes, were observed to have resulted in the same structural changes in the synthesized material. The same average hardness values were found for the samples of both routes and the gathered XRD patterns were found to be similar, etc. Among the compacts of both route consolidations, explosively consolidated "double tube design compacts" were determined to possess the most desirable, most uniform and well established characteristics after the consolidation, densification sintering and also aluminum infiltration steps. In addition to the above stated argument, it was observed that the sample hot pressed for 2 h had better properties than the single tube design consolidated body, whereas, the sample hot pressed for 4 h had better mechanical properties than the former two.

Considering the bulk density, microhardness, apparent and closed porosity, fracture toughness and flexural strength values of the aluminum infiltrated compacts, 1200 °C was determined as the optimum aluminum infiltration temperature for the boron suboxide (matrix)-aluminum system (see Tables II–VI).

The proposed intent of the study, the production of aluminum infiltrated boron suboxide drag cutters and drill bits [with fracture toughness values of 5–6 MPa $m^{1/2}$ (rivaling that of tungsten carbide, 7–23 MPa $m^{1/2}$), hardness values of 38–40 GPa (rivaling that of polycrystalline diamond, 50 GPa) and temperature stabilities of higher than 1800 °C that dramatically exceed that of polycrystalline diamond (PDC) cutters (350/750 °C)] was accomplished.

Acknowledgements

Support for this research has been given by Sandia National Laboratories (SNL), Albuquerque, through contract # AV4630 and is gratefully acknowledged.

References

1. A. R. BADZIAN, *Appl. Phys. Lett.* **53**(25) (1988) 2495–2497.
2. "VIII Borides of Group VI b Elements," *Boron and Refractory Borides*, edited by V. I. Matkovich and G. L. Gal'Chenko *et al*. (Springer-Verlag, Berlin, 1977) pp. 331–333.
3. H. F. RIZZO, W. C. SIMMONS and H. O. BIELSTEIN, *J. Electrochem. Soc.* **109** (1962) 1079–1082.
4. M. A. MEYERS and S. L. WANG, *Acta Metall.* **36**(4) (1988) 925–936.
5. C. TOY and W. D. SCOTT, *J. Amer. Ceram. Soc.* **73**(1) (1990) 97–101.

Received 9 December 1998
and accepted 15 March 1999